Hindawi
Geofluids
Volume 2023, Article ID 3492686, 12 pages
https://doi.org/10.1155/2023/3492686

Research Article

Roadway Instability Mechanism of Weakly Consolidated Soft Rocks and Support Technologies

Jinlong Cai,[1,2] **Min Tu**,[2] **Luxiu Chai**,[1] **Fengyan Qin**,[1] **and Zhengfeng Shen**[1]

[1]*School of Architecture and Civil Engineering, West Anhui University, Lu'An, Anhui 237012, China*
[2]*Key Laboratory of Safe and Effective Coal Mining, Ministry of Education, Anhui University of Science and Technology, Huainan, Anhui 232001, China*

Correspondence should be addressed to Min Tu; mtu@aust.edu.cn

Received 4 April 2022; Revised 15 September 2022; Accepted 12 October 2022; Published 3 March 2023

Academic Editor: Mohammed Fattah

During tunneling in weakly consolidated soft rock strata, lithology, joints, and fractures of rock strata play an important role in controlling overall roof stability of the roadway. A case study based on weakly consolidated soft rock roadway in Bojianghaizi mine was conducted to address disasters caused by sudden changes and collapse as well as difficulties in maintenance of weakly consolidated soft rock roadway. First, physical and mechanical properties of weakly consolidated soft rocks were investigated by X-ray diffraction mineral component analysis and scanning electron microscopy. Second, failure characteristics and instability mechanism of the roadway were analyzed by combining field survey and theoretical analysis. A mechanical model of fracture development on the composite roof of the roadway was built, and the initiation angle and critical stress for fracture development were deduced. The instability criteria of cracks based on cracking angle (θ_0) were established. Moreover, the instability mechanism caused by roof falling was disclosed. Fractures were formed upon shear failure at vertex angle of the roadway. The fracture belt extended to the soft bedding plane of the separation stratum along the fracture propagation angle and connected with it, thereby inducing roof falling. On this basis, a high-strength and high-preload "inverted trapezoidal" anchoring mesh-beam string supporting structure + arched roadway cross-section with vertical walls + full-section guniting coupling control technology was proposed, which achieved good site application effects.

1. Introduction

With the gradual exploitation of coal resources in mideastern China, the coal resource exploitation center has gradually shifted to the midwestern region. Owing to squeezing influences by the Qinghai–Tibet subplate, North China plate, and Tarim plate against coal-measure strata in midwestern China, extensive weakly consolidated soft rock strata exist in the local coal-measure strata [1–3], which are mainly manifested by low strength of surrounding rocks, poor cementing properties, weathering swelling upon water, and easy development of separation stratum among different rock strata. In these geological conditions, the excavated roadway is characterized by great deformation, high deformation rate with a long duration, which increases the difficulties in roadway support.

During tunneling in weakly consolidated strata, relatively high development of fractures and joints occurs during the advancing and follow-up service periods. When the roadway roof bears stresses, a great tensile stress occurs in the lower part, which can easily cause uneven subsidence. Moreover, weak interlayer adhesive forces exist due to the complicated roof structure, which easily develops an extreme separation stratum. The space domain of this separation stratum shifts quickly from progressive extension to sudden changes and roof falling-induced disasters, thereby causing accidents on weakly consolidated soft rock roadways [4, 5]. Many experts and scholars in China and other countries have conducted theoretical and experimental studies to address sudden changes and roof falling-induced disasters of weakly consolidated soft rock roadways as well as difficulties in maintenance control. For example, Zhang and Jiang

[6], Zhang et al., Zhao et al, and Jia et al. [7–9] studied bending-induced instability mechanism of stratified roof separable strata in a coal roadway and pointed out that it could easily cause shearing stress concentration at the vertex angle due to stratified roof separation and bending, which further extended to the upper hard rock strata and intensified the risks of roof falling. Zhang et al., Guo et al., and Cao et al. [10–12] established the systematic mechanical model of the rock composite system, which contains interlayers to disclose the failure and instability mechanism of surrounding rocks in roadways with interlayer rocks and determine judgment indexes for surrounding rock stability. Research results provided references for the control design of stratified rock stability. Considering the stratified roof structural characteristics of full-coal roadway with a large cross-section, Zhang et al. [13, 14] investigated the deformation characteristics of the separation layer on a stratified roof after tunneling by using state nonlinear simulation method of interlayer contact surfaces. Based on analysis of the deformation failure characteristics of soft rock roadway, Meng et al. [15–17] studied the deformation failure mechanism of surrounding rocks in weakly consolidated soft rock roadway; they also investigated and supervised surrounding rock evolution laws in the roadway as well as optimized support design. Li et al. [18] analyzed the deformation failure process of rectangular roadway of weakly consolidated soft rocks and compared simulation results with field supervision results. Some suggestions in cross-section shape selection and roadway support were provided. Li and Hou [19] pointed out that a semicircle arched roadway with vertical walls and anchoring mesh-beam spraying supporting structure could improve the physical and mechanical properties of surrounding rocks effectively and increase the bearing capacity of surrounding rocks.

Although relevant experts and scholars have investigated the deformation failure characteristics and mechanism of the soft rock roadway, the deformation failure characteristics of the weakly consolidated soft rock roadway are different from those of the ordinary soft rock roadways. This is still in the exploration stage at present. Based on mineral composition, space characteristics, and microscopic structure of weakly consolidated soft rocks, this study further explores the internal deformation instability mechanism of the roadway and established theoretical criteria of roof instability. Research conclusions provided theoretical references to the design of the roof support scheme of a weakly consolidated roadway.

2. Engineering Overview and Lithologic Characteristics

2.1. Engineering Overview. The Bojianghaizi coal mine is located in Dongsheng District, Inner Mongolia. The first working face was 113101, which was advanced by 2603 m. The surface length and mining area were 200 m and 520,600 m^2, respectively. Coal seam #3-1 was stable and belonged to a uniclinal and approximately horizontal structure. The thickness of this coal seam was 3.2–6.4 m, averaging at 5.4 m. The basic roof was medium-coarse sandstone, and the average thickness was 7.07 m. The direct bottom was sandy mudstone, and the old bottom was 5 m thick siltstone. The geological location is shown in Figure 1.

The working face 113101 has been the site of roof falling accidents. The length and maximum height of the roof falling section were 14.6 m and 10.2 m, respectively. The roof falling region resembles an upside-down bowl and is narrow in the upper part and wide at the bottom. Four holes were drilled on the roof in this region by using a SGZ-IIIA drill for roof detection. The profiles of field drilling and survey diagram are shown in Figure 2.

According to comprehensive analysis, the roadway roof was composed of crushed rock section (0–3 m), grouting section (3–6 m), empty roof section (6–10.2 m), and hard roof (>10.2 m). Therefore, the maximum height of roof failing was 10.2 m, and the maximum distance of the empty roof was 7.2 m. Comprehensive analysis of drilling shows that lithology in the section of the roof falling zone from the upper part to the bottom is coal, thin mudstone layer with coal lines, fine sandstone, and sandy mudstone. The lithology is brittle, and the full section is generally horizontal. The cable anchoring section is basically made up of sandy sandstones. Obvious fracture surfaces and buried structures exist in the falling roof. Vertical fracture developments are on the sides, which lead to poor shaping of the roadway before and after the roof falling and serious wall caving. In particular, the maximum wall caving at the shoulder reaches as high as 1.5 m. In view of field drilling detection on the roof, the roof falling thickness is in the 6–6.5 m range. In other words, the weak strata or interlayers fall completely except for the effective supporting scope of anchoring cables.

2.2. Analysis of Lithologic Characteristics. The minable seams mainly distribute in Jurassic and Cretaceous strata. The average uniaxial compressive strengths of fine siltstone and sandy mudstone in surrounding rocks of the roadway are 29.9 MPa and 24.1 MPa, respectively. The average uniaxial compressive strength of the sandy mudstone changes to 7.8 MPa after softening by water absorption, and the softening coefficient reaches 0.32.

Four rock samples were collected from the roof and floor of coal seams, which were sandstone and sandy mudstone. XRD analysis was conducted on all rock samples. The XRD spectra of the sandstone and sandy mudstone are shown in Figure 3. Quartz, feldspar, illite, kaolinite, and chlorite are major mineral components. In view of the microstructural characteristics of rocks under SEM (Figure 4), sand structures form porous cementation and the skeleton structure is a characteristic of porous, stacking, and loosing. Fine clays are arranged randomly, which are off-white and have moderate roundness. They present subangular and semiround shapes and have uneven sizes and clear edges.

In other words, the microstructures of weakly consolidated rocks are cellular, with uneven particles stacking together. A large number of pores bring good connectivity. The whole structure is relatively weak and exhibits low rock strength. Clay minerals are dominant, and kaolinite accounts for the highest proportion, which is characterized by easy swelling and disintegration in water.

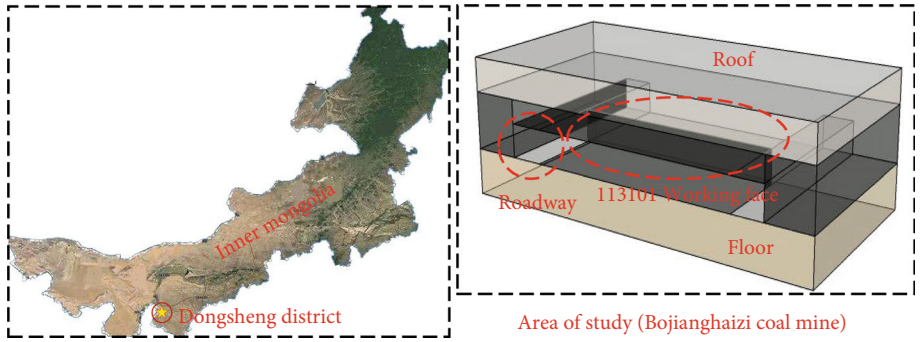

Figure 1: Roadway research geographical location.

3. Instability Mechanism and Mechanical Analysis of Weakly Consolidated Soft Rocks

Stresses in the upper roof strata are released after tunneling. Due to collaborative action of compressive, tensile, and shear stresses, different strata have varying deformations. Evident separation is developed between any two strata, and the roof is further bent. Fractures are formed at the vertex angle of the roadway.

3.1. Stress Field Analysis at Fracture Tip

3.1.1. Stress Distribution and Strength Factor at the Tip of Compression Shear Fracture. Figure 5 shows that the initial fracture is 2a long. Influenced by a combination of the vertical stress (σ_y) and horizontal stress (σ_x), normal and tangential stresses on the fracture surface can be obtained as follows:

$$\begin{cases} \sigma_n = \sigma_y \sin^2\beta + \lambda\sigma_y \cos^2\beta, \\ \sigma_n = -\sigma_y(1-\lambda)\sin\beta\cos\beta, \end{cases} \tag{1}$$

where σ_n and τ_n are positive stress and tangential stress on the fracture surface, respectively, and λ is the lateral pressure coefficient.

In this case, the stress strength factor at the crack tip is [20]

$$\begin{cases} K_{\mathrm{I}} = -\sqrt{\pi a}\sigma_y\left(\sin^2\beta + \lambda\cos^2\beta\right), \\ K_{\mathrm{II}} = \sqrt{\pi a}\sigma_y(1-\lambda)\sin\beta\cos\beta. \end{cases} \tag{2}$$

3.1.2. Stress Distribution and Strength Factor at the Tip of Tensile Shear Fracture. As the practical loads on the roof rock beam are usually uneven, strength factor could be calculated by the integral method under these circumstances [20]. Results are shown in Figure 6.

In this case, the stress strength factor at the tip of cracks is

$$\begin{cases} K_{\mathrm{I}} = \dfrac{1}{2\sqrt{\pi}}\displaystyle\int_{-a}^{a} p(x)\sqrt{\frac{a+x}{a-x}}d(x) + \frac{1}{2\sqrt{\pi}}\left(\frac{k-1}{k+1}\right)\int_{-a}^{a} q(x)d(x), \\ K_{\mathrm{II}} = \dfrac{1}{2\sqrt{\pi}}\displaystyle\int_{-a}^{a} q(x)\sqrt{\frac{a+x}{a-x}}d(x) - \frac{1}{2\sqrt{\pi}}\left(\frac{k-1}{k+1}\right)\int_{-a}^{a} p(x)d(x), \end{cases} \tag{3}$$

where

$$k = \begin{cases} \dfrac{3-\nu}{1+\nu}, & \text{Plane stress,} \\ 3-\nu, & \text{Plane strain,} \end{cases} \tag{4}$$

where ν is Poisson's ratio.

(1) Horizontally, the rock beam at the upper position of the roadway bears upward and downward linear positive stresses, as shown in Figure 7

At this moment, the strength factor could be calculated as follows:

$$\begin{cases} K_{\mathrm{I}} = \dfrac{\sigma_x}{2}\sqrt{\pi a}\cos^2\beta, \\ K_{\mathrm{II}} = \dfrac{\sigma_x}{2}\sqrt{\pi a}\sin\beta\cos\beta. \end{cases} \tag{5}$$

(2) Vertically, the rock beam at the upper position of the roadway bears leftward and rightward linear shear stresses. In this case, the stress analysis of inclined cracks is shown in Figure 8

Thus, the stress strength factor can be obtained as follows:

$$\begin{cases} K_{\mathrm{I}} = \dfrac{2\tau_{\max}a(\pi-2)}{\sqrt{\pi a}}\sin\beta\cos\beta, \\ K_{\mathrm{II}} = \dfrac{\tau_{\max}a(\pi-2)}{\sqrt{\pi a}}\cos 2\beta. \end{cases} \tag{6}$$

3.1.3. Composite Fractures under Collaboration of Multiple Stresses. Unit blocks in the rock beam of the rectangular roadway roof are subordinated to the collaborative effect of multiple stresses. According to stress superposition principle [21], the strength factor of composite fracture was calculated by using the stress superposition method (Figure 9).

According to literature [22], then the tensile stress acts on the crack surface; the initial cracks are damaged by tensile stress and then become extensive cracks. According to the

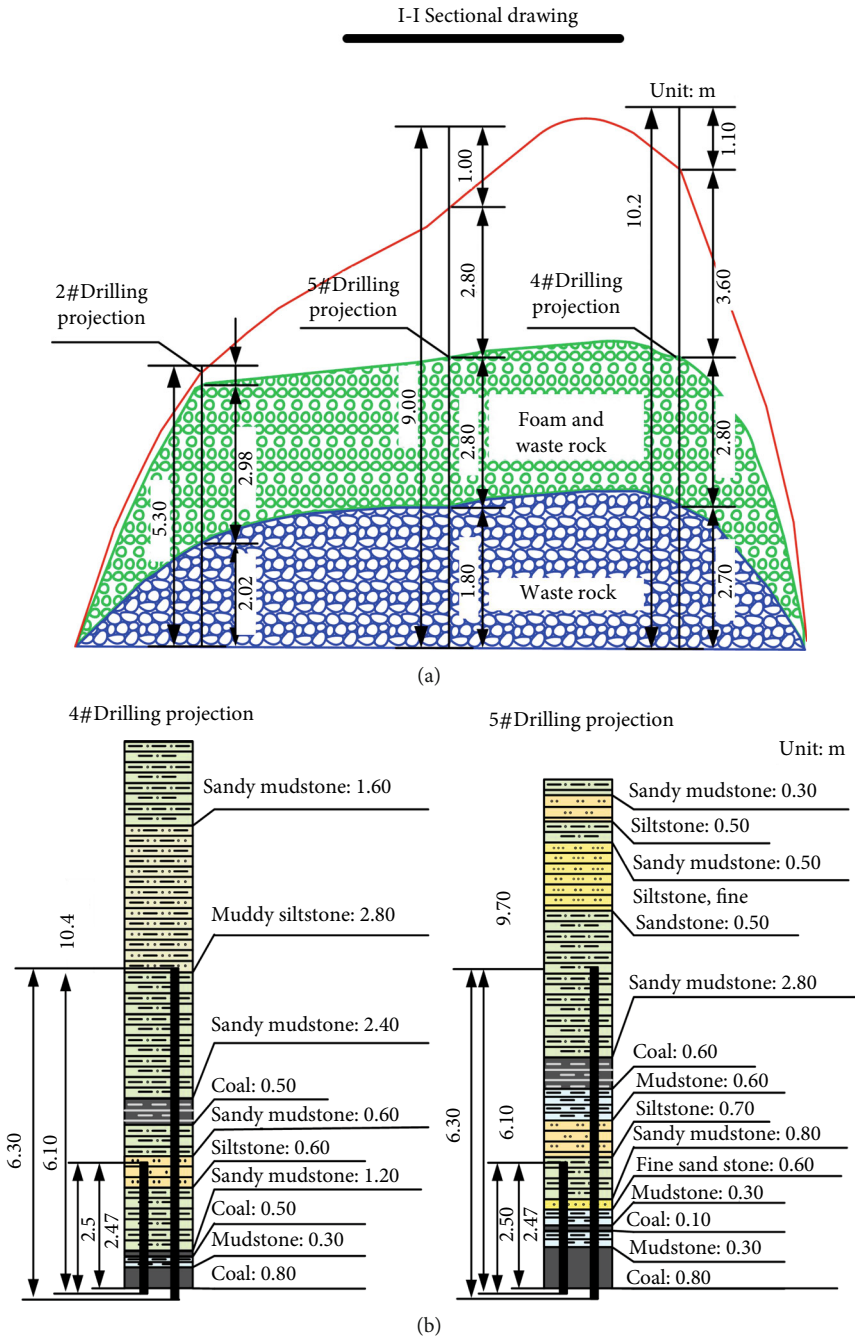

Figure 2: The diagrammatic cross-section of caving zone: (a) the schematic diagram of drilling section; (b) the columnar section of investigation.

preceding analysis results, Equations (2), (5), and (6) were combined to calculate the composite strength stress factor:

$$\begin{cases} K_{\mathrm{I}} = \dfrac{\sigma_{\max}}{2}\sqrt{\pi a}\cos^2\beta + \dfrac{2\tau_{\max}a(\pi-2)}{\sqrt{\pi a}}\sin\beta\cos\beta, \\ K_{\mathrm{II}} = \dfrac{\sigma_{\max}}{2}\sqrt{\pi a}\sin\beta\cos\beta + \sqrt{\pi a}\sigma_y(1-\lambda)\sin\beta\cos\beta - \dfrac{\tau_{\max}a(\pi-2)}{\sqrt{\pi a}}\cos 2\beta. \end{cases} \tag{7}$$

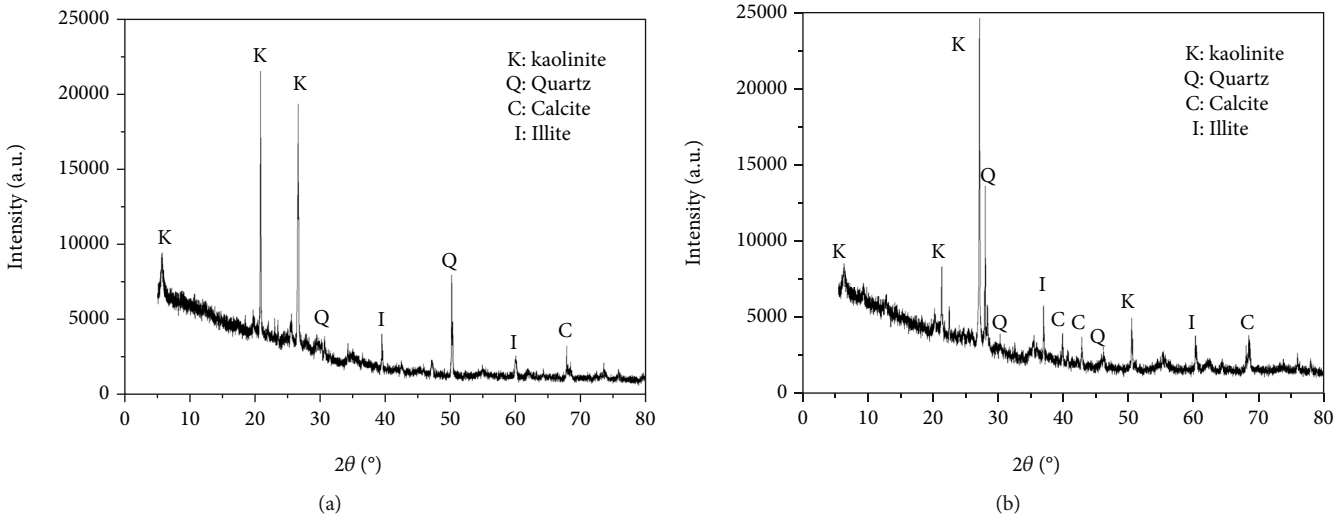

Figure 3: The results of XRD: (a) medium sandstone; (b) sandy sandstone.

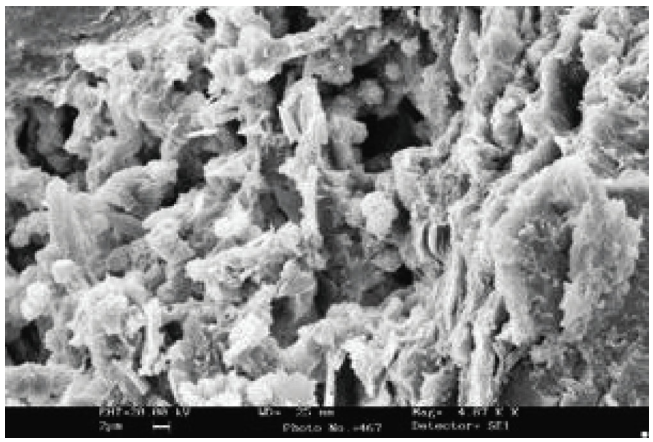

Figure 4: Microstructure of rock.

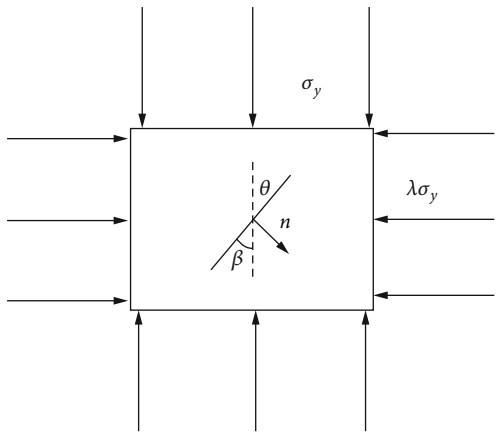

Figure 5: Schematic diagram of expansion of compression shear crack tip.

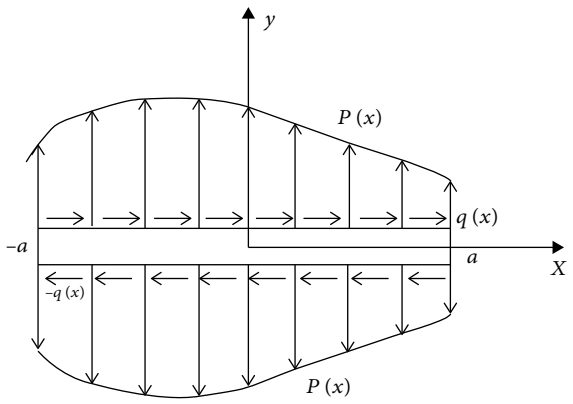

Figure 6: Schematic diagram of expansion of compression tensile shear crack tip.

According to mechanical related knowledge of materials, $\sigma_{\max}$ and $\tau_{\max}$ can be expressed as follows:

$$\begin{cases} \sigma_{\max} = \dfrac{M'}{W_z} = \dfrac{6\left(M + (ql/2)x - (1/2)qx^2 + p\omega\right)}{bh^2}, \\ \tau_{\max} = \dfrac{3F_s}{2bh}. \end{cases} \tag{8}$$

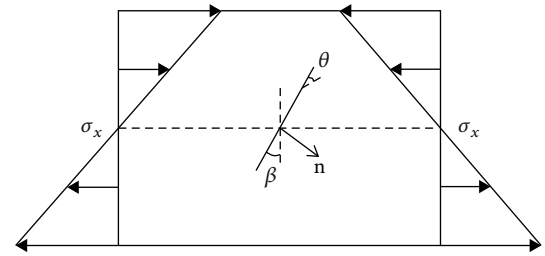

Figure 7: Schematic diagram of fracture tip expansion in horizontal direction of rock beam.

Equations (7) and (8) were combined as follows:

$$\begin{cases} K_{\mathrm{I}} = \dfrac{3\left(M + (ql/2)x - (q/2)x^2 + p\omega\right)}{bh^2}\sqrt{\pi a}\cos^2\beta + \dfrac{3F_s}{bh}\dfrac{a(\pi-2)}{\sqrt{\pi a}}\sin\beta\cos\beta, \\ K_{\mathrm{II}} = \dfrac{3\left(M + (ql/2)x - (q/2)x^2 + p\omega\right)}{bh^2}\sqrt{\pi a}\sin\beta\cos\beta + \sqrt{\pi a}\sigma_y(1-\lambda)\sin\beta\cos\beta - \dfrac{3F_s}{2bh}\dfrac{a(\pi-2)}{\sqrt{\pi a}}\cos 2\beta. \end{cases} \tag{9}$$

3.2. Composite Breakage Criteria. In practical engineering, almost all fractures are composite type. Many experts and scholars in China and other countries have conducted numerous studies on the judgment of crack expansion direction and critical loads of expansion. Among them, the maximum circumferential stress criteria are used mostly [23], which posit the following:

(1) When $(\sigma_\theta)_{\max}$ reaches the critical value σ_c, cracks begin to propagate

(2) The propagation direction of composite crack is the direction when σ_θ is the maximum

Based on the aforementioned criteria, the initiation angle θ_0 of cracks is

$$\theta_0 = \arcsin\frac{1}{\sqrt{(K_1/K_2)^2 + 9}} - \arctan\frac{3K_{\mathrm{II}}}{K_{\mathrm{I}}}. \tag{10}$$

The critical value of maximum circumferential stress $(\sigma_\theta)_c$ is

$$(\sigma_\theta)_c = \frac{K_{\mathrm{IC}}}{\sqrt{2\pi a}} = \frac{\cos(\theta_0/2)\left[K_{\mathrm{I}}\cos^2(\theta_0/2) - (3/2)K_{\mathrm{II}}\sin\theta_0\right]}{\sqrt{2\pi a}}. \tag{11}$$

3.3. Analysis of Fracture Propagation Parameters on Roadway Roof. The composite roof of weakly consolidated soft rock roadway in the first working face of the Bojianghaizi mine was used in the case study. The breakage criteria applied the maximum circumferential stress criteria. The first working face of the Bojianghaizi mine was at 540 m underground, and the net section size of the rectangular roadway was $b = 5.6$ m in width and $h = 3.6$ m in height. According to the primary stress and experimental test, vertical stress, lateral pressure coefficient, Poisson's ratio of rocks, initial cracking angle of rock beams, and uniformly distributed loads on beams were $\sigma_y = 14$ MPa, $\lambda = 0.8$, $\mu = 0.25$, $\beta = 5°$, and $q = 500$ kPa, respectively. The above numerical values were brought into Equations (10) and (11), which lead to the data in Figures 10–14.

Figure 10 shows that with the increase of strata thickness, the positive and shear stresses on the fractures decrease gradually. The fracture development angle in the strata decreases, and the fractures present small-angle development. Under this circumstance, the critical stress of fracture development also declines. When the lithology of the upper rock beam of the roadway is relatively weak, the bending and sinking rock beam thickens and the direct roof of the roadway easily develops connected fractures, thereby leading to roof falling accidents. Thus, a supporting structure has to be designed reasonably to prevent fracture propagation.

Figure 11 shows that with the increase of distance to the ends of rock beams, the fracture propagation angle decreases and the critical stress increases. In other words, fractures at the ends of the rock beam are easier to propagate toward large angles. Thus, an inclined anchor rod or cable has to be applied at two ends of the roadway roof to prevent crack propagation.

Figure 12 shows that with the increase of distance to the ends of rock beams, the fracture propagation angle decreases and the critical stress increases. In other words, fractures at the ends of the rock beam are easier to propagate toward large angles. Thus, an inclined anchor rod or cable has to be applied at two ends of the roadway roof to prevent crack propagation.

As shown in Figure 13, the fracture development angle increases gradually with the increase of the lateral pressure coefficient, while the critical stress declines gradually. This result reveals that with the increase of horizontal stress, the risk of high-angle falling of the rock beam also increases.

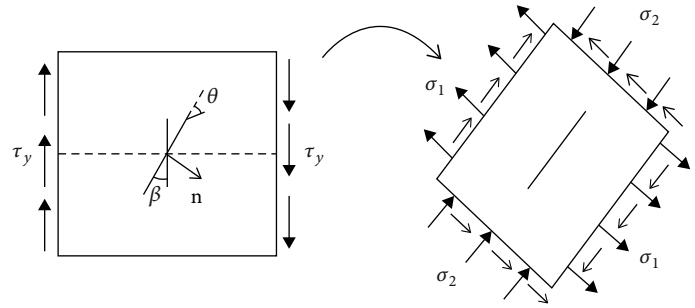

Figure 8: Schematic diagram of fracture tip expansion in level direction of rock beam.

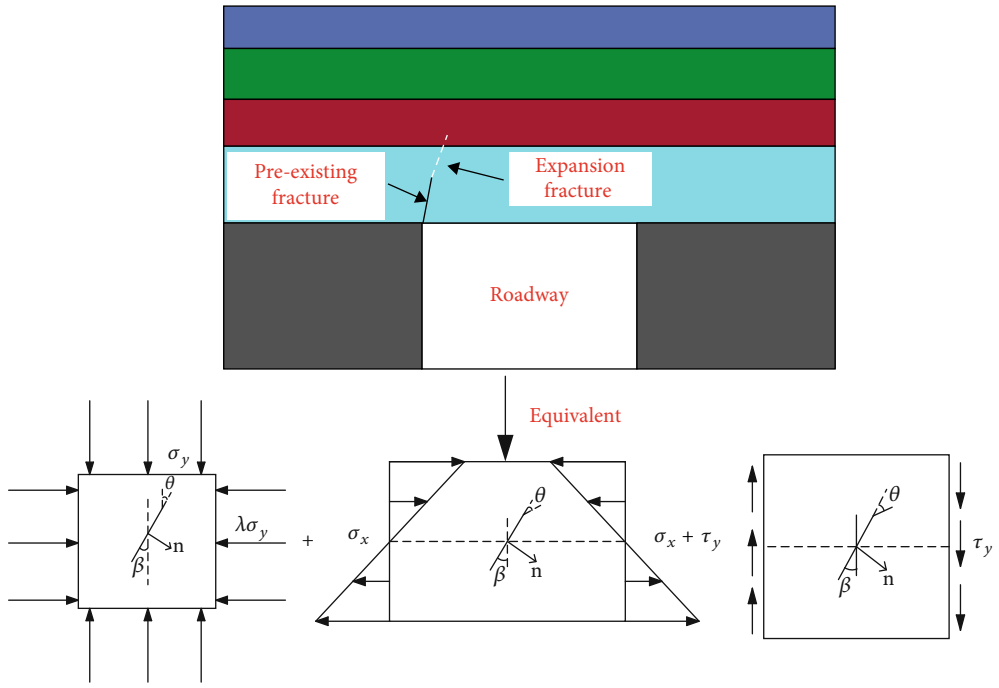

Figure 9: Equivalent diagram of composite fracture strength factor.

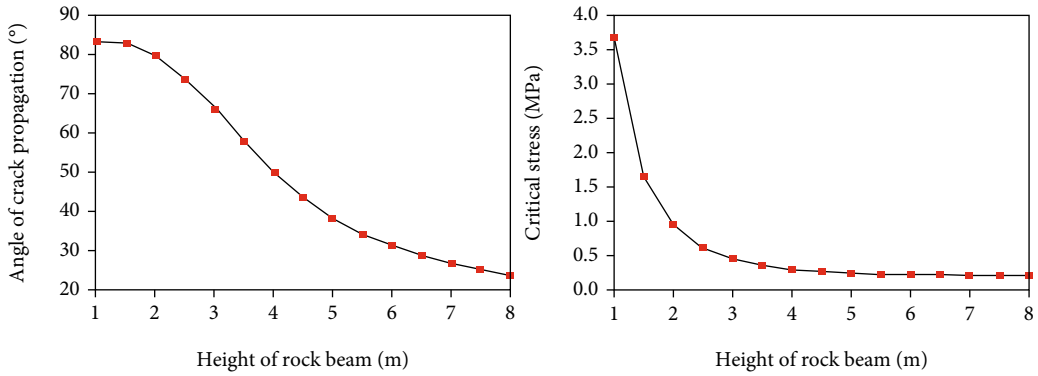

Figure 10: Sensitivity analysis of crack propagation angle and critical stress and rock beam height.

4. Instability Mechanism Analysis of Roadway Roof

The weakly consolidated roof has thin layers, and the interlayer cohesive force is weak. The roof begins to bend and sink in response to the gravity of overlying stones and horizontal stresses, thereby generating a shear force. Shear dislocation occurs between layers when the shear force is larger than the interlayer shear resistance. When the flexural rigidity of the lower rock strata is higher than that of the upper rock strata, it maintains coordinated movement and the layer separation is not obvious; otherwise, the layers are

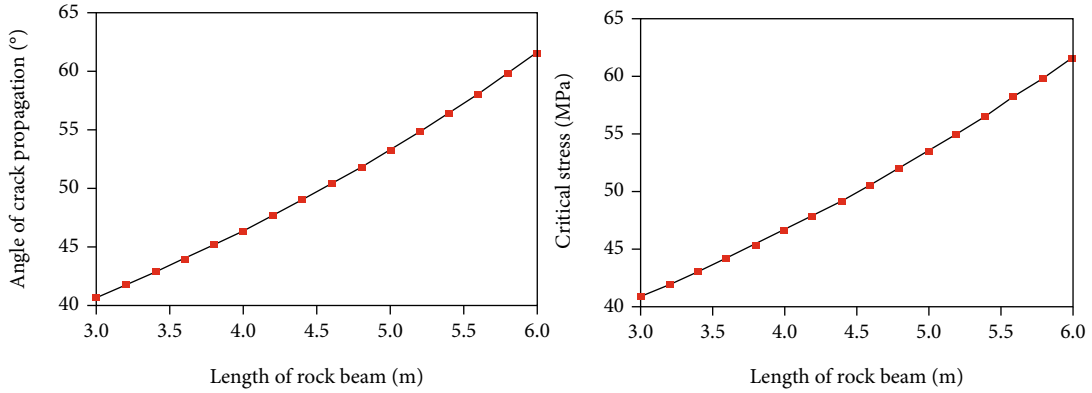

Figure 11: Analysis of crack propagation angle and critical stress and length of rock beam.

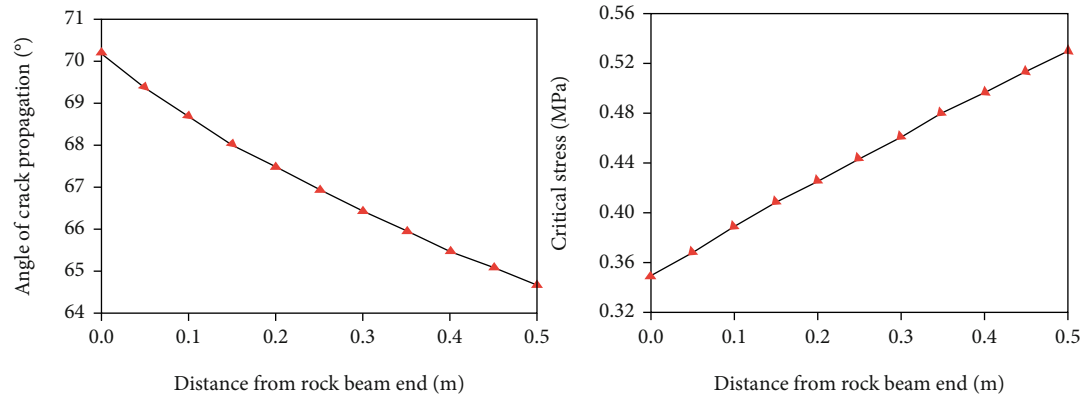

Figure 12: Analysis of crack propagation angle and critical stress and sensitivity of distance beam end.

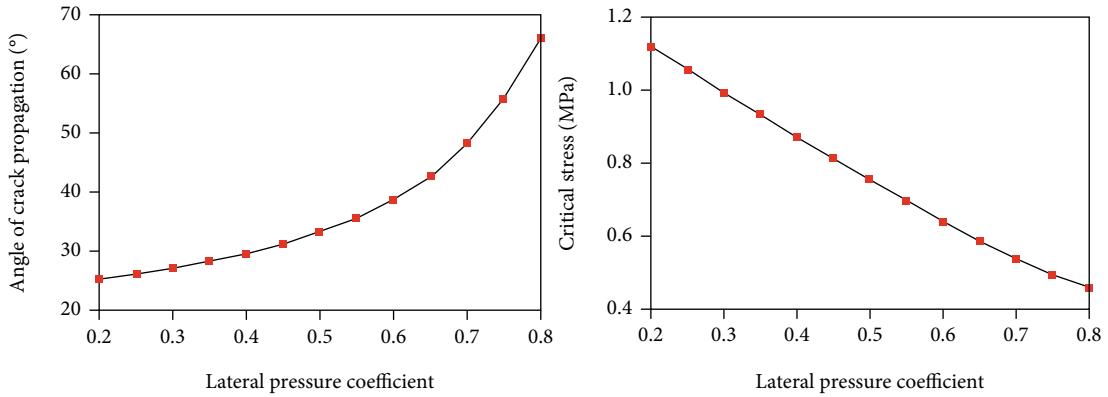

Figure 13: Sensitivity analysis of crack propagation angle and critical stress and lateral pressure coefficient.

separated. With the increase of layer separation, the roof is further bent and great shear stress is easily generated at the vertex angle of the roadway. Shearing failure occurs when this shear stress exceeds the shear strength of the rocks on the roof. When the shear failure forms cracks at the vertex angle of the roadway, this crack belt extends upward at an angle to the deep rock strata. Subsequently, the crack belt connects with the soft bedding plane of the separation stratum or soft weak interlayer, thus inducing roof falling. This process is shown in Figure 14.

According to instability mechanism analysis, the thin-layered roof is bent and deformed due to the dual actions of dead loads and horizontal stress of the roadway, thereby generating shear stress concentration at the vertex angle and causing shear failure. Cracks are formed at the vertex angle of the roadway. This crack belt extends upward along the fracture propagation angle to the soft bedding plane of the separation stratum of the soft weak interlayer and then connects with them, finally causing roof falling.

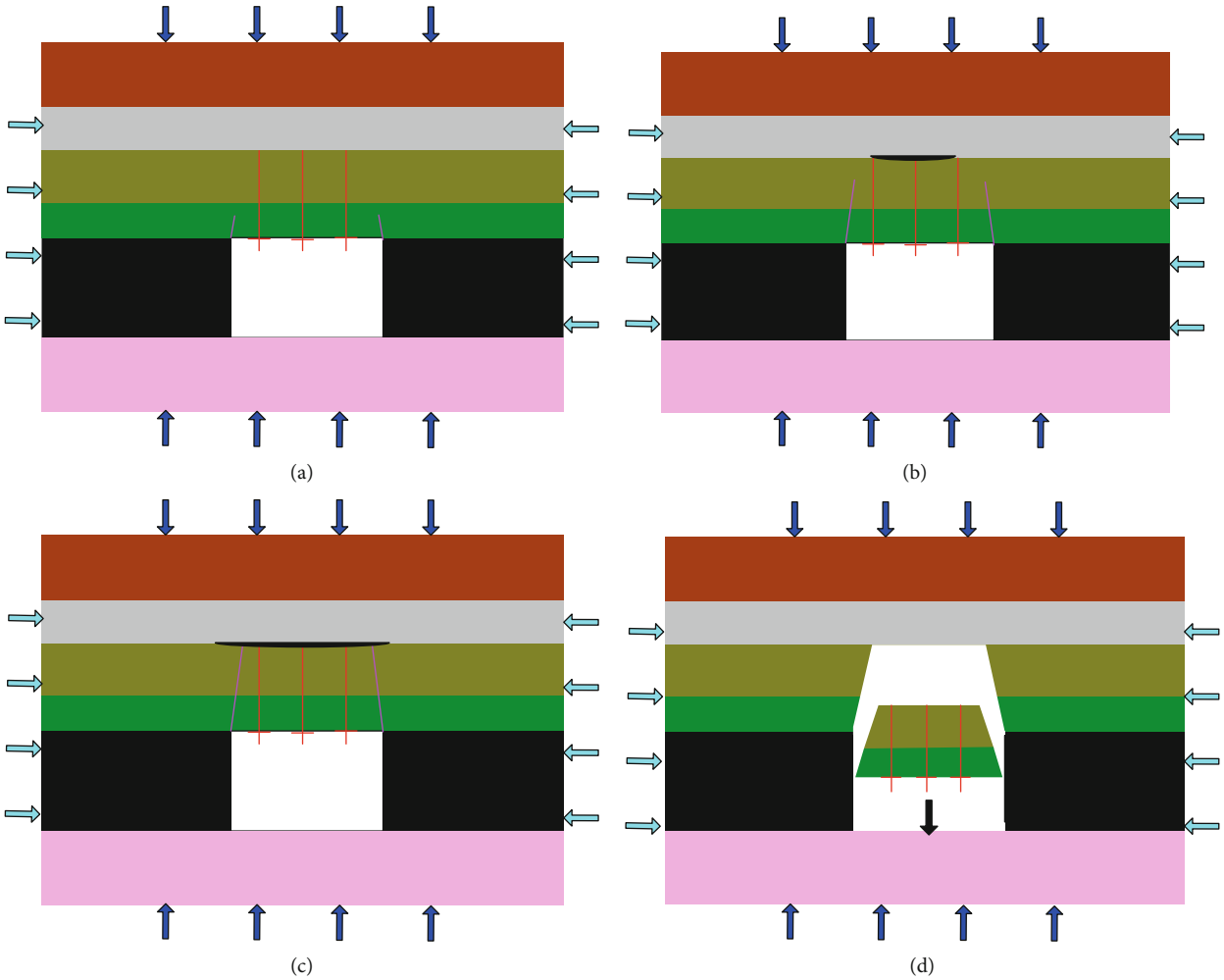

Figure 14: Evolution process of roof caving: (a) crack produce; (b) crack development; (c) fracture penetration; (d) roof caving.

5. Surrounding Rock Control and Engineering Applications

5.1. Roadway Control Technology. Due to the collaborative influences of primary deposit and diagenesis of weakly consolidated soft rock roadway, the degree of consolidation of rock strata is low, accompanied with poor cementation or rocks and weak interlayer adhesive force. Rocks have low compressive and tensile strengths. Due to tectonic lifting effect in the late stage, vertical and tensile fractures are extensively developed in rock strata, thus making rocks brittle and easy to crash. Based on the preceding analysis, the key to control deformation and instability of weakly consolidated soft rock roadways is to maintain the continuity of rock beams on the stratified roof and prevent softening of the weak interlayer or bedding plane above the anchoring body, controlling the separation layers and inhibiting the vertex angle failures of the roadway.

To overcome the deformation failures of weakly consolidated soft rock roadway, this study proposes a high-strength and high-preload "inverted trapezoidal" anchoring mesh-beam string supporting structure + arched roadway cross-section with vertical walls + full-section guniting coupling optimization support structure (Figure 15). The self-bearing capacity of surrounding rocks is used fully, which not only allows deformation of surrounding rocks but also restricts deformation. The roof becomes increasingly stable in the process of collaborative action of surrounding rocks and anchoring supporting structure.

5.2. Engineering Applications. To verify the reliability of supporting technology after the optimization, this study examines the applications of this technology during field experiment in the return roadway of working face #113102 in coal seam #3-1. To further elaborate the effects of optimized supporting scheme in the separation and deflection control of the roof, the internal structure of the roadway roof was studied by using a TS-C0601 drill imager after the roadway was advanced for 10 months. Results are shown in Figure 16.

Through the drill imaging, white cracks were detected near 1.6 m in the upper position of the roof, which were separation layers. The separation layer size was approximately 6–7 mm. Furthermore, an annular black zone within a certain scope occurred on the porous wall, which is 6.2 m near the upper position of the roof, and the separation layer size

Main technical data:
Tunnel cross-section: Width × Height = 5.6 m × 3.6 m;
The bolt spacing of roof bolt: 850 mm × 900 mm;
The bolt spacing of roadway gang:
900 mm × 900 mm;
Cable interval: 1400 mm;
Top bolt: Φ22 × 2500 mm;
Gang bolt: Φ20 × 2000 mm;
Cable: Φ17.8 × 8300 mm;
U-bar: 12#;
Metal net: 8# wire fence;
Steel belt of roadway gang: W3;
Pre-tightening force of anchor cable: 150 KN;
Installation depth of anchor cable: 8300 mm;

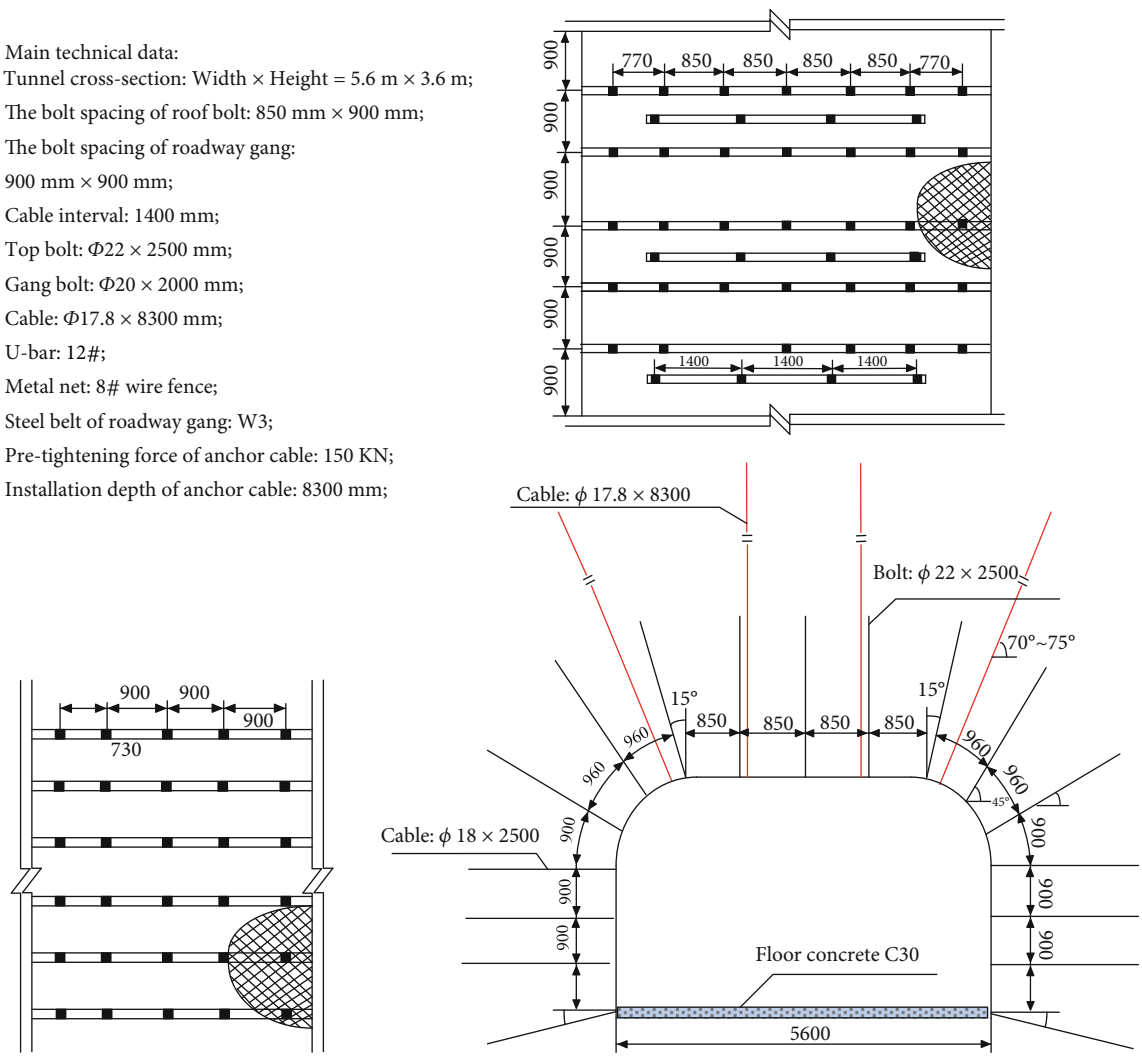

Figure 15: The new support parameter of the soft-rock coal roadway.

(a) (b)

Figure 16: Roof borehole peep view: (a) 1.6 m; (b) 6.2 m.

was approximately 7–10 mm. In the experimental section, surrounding rocks on the roadway roof were relatively integrals, without evident opening bedding and the separation value of the roof was small. Cracks were not connected yet, which further proved that the optimized supporting structure could effectively control the separation layers, fracture development, and roof connection, thereby improving the overall structure of the roof.

6. Conclusions

(1) According to the laboratory test of mineral composition and structural analysis of the roof, the weakly consolidated rocks generally form a weak structure and have low rock strength. Moreover, clay minerals are the major mineral components. Kaolinite accounts for the highest proportion and is a characteristic of swelling and disintegration in water

(2) The mechanical model of fracture development in the composite roof of the roadway is constructed, thereby obtaining the initiation angle and critical stress of fracture development. The critical cracking angle (θ_0) of the roof is obtained according to the strain energy density factor of crack propagation

(3) Through an engineering case study, relations of rock beam height, span of roadway, and fracture development angles at the ends of rock beams with fracture development trend and critical stress of crack propagation are disclosed. On this basis, the instability mechanism of roof falling in the roadway is summarized. Shear failure occurs at the vertex angle of the roadway, thereby forming cracks. The crack belt extends along a certain angle to the soft bedding plane of the separation stratum or weak bedding plane and finally connects with them, which leads to roof falling

(4) A high-strength and high-preload "inverted trapezoidal" anchoring mesh-beam string supporting structure + arched roadway cross-section with vertical walls + full-section guniting coupling optimized supporting structure is proposed to solve the deformation failure of weakly consolidated soft rock roadway. According to field test results, this optimized supporting structure can effectively control the separation and deformation of the roadway, thereby significantly increasing the stability of surrounding rocks

Data Availability

The data used to support the findings of this study are included within the article.

Conflicts of Interest

The authors declare that there is no conflict of interest regarding the publication of this article.

Acknowledgments

This research was funded by the Open Research Fund Project of Key Laboratory of Safety and High-Efficiency Coal Mining of Ministry of Education of the People's Republic of China (JYBSYS2021202), the research start-up fees for high-level talents of West Anhui University (WGKQ2021071), the Domestic Study Visit and Training Project for Outstanding Young Backbone Teachers in Colleges and Universities in Anhui Province (gxgnfx2020096), and the Provincial Quality Engineering Project of colleges and universities of Anhui Provincial Department of Education (2020jyxm2153 and 2020szsfkc0953).

References

[1] H. B. Jia, L. J. Su, and Z. Qin, "Ground stress numerical inversion of roadways with weakly cemented strata," *Chinese Journal of Shandong University of Science and Technology (Natural Science)*, vol. 30, no. 5, pp. 30–35, 2011.

[2] Q. B. Meng, L. J. Han, W. G. Wei, D.-G. Lin, and J.-D. Fan, "Evolution of surrounding rock in pioneering roadway with very weakly cemented strata through monitoring and analyzing," *Chinese Journal of Coal Society*, vol. 38, no. 4, pp. 572–579, 2020.

[3] W. M. Wang, L. Wang, and C. Q. Dai, "Frozen wall deformation analysis in weakly cemented soft rock based on layered calculation of strength," *Chinese Journal of Rock Mechanics and Engineering*, vol. 30, no. 5, pp. 4110–4116, 2011.

[4] Q. F. Zhao, N. Zhang, G. Z. Li, and R. Peng, "Similarity simulation experimental study on abrupt collapse of roof separation in large cross-section argillaceous roadway," *Chinese Journal of Mining & Safety Engineering*, vol. 35, no. 6, pp. 1107–1115, 2018.

[5] N. Zhang and L. Yuan, "Control principle of separating and broken roof rock strata in roadway," *Chinese Journal of Mining & Safety Engineering*, vol. 23, no. 1, pp. 34–38, 2006.

[6] N. Zhang and Y. Jiang, "Theoretical estimation of loosening pressure on tunnels in soft rocks," *Chinese Journal of Tunneling and Underground Space Technology*, vol. 16, no. 2, pp. 99–105, 2001.

[7] N. Zhang, Z. C. Zhang, J. B. Bai, W. J. Wang, and H. Wu, "Mechanical analysis of roof separation within and outside anchorage zone above backfill area of gob-side entry retaining and its engineering application," *Chinese Journal of Mining & Safety Engineering*, vol. 35, no. 5, pp. 893–901, 2018.

[8] Z. H. Zhao, N. J. Ma, H. T. Liu, and J. C. Feng, "Mechanism and early-warning methods of roadway roof fall in coal seam," *Chinese Journal of Coal Society*, vol. 43, no. 2, pp. 369–376, 2018.

[9] H. S. Jia, G. S. Li, L. Y. Wang, and A. Z. Qiao, "Characteristics of stress-field environment and roof falling mechanism of mining influenced roadway," *Chinese Journal of Mining & Safety Engineering*, vol. 34, no. 4, pp. 707–714, 2019.

[10] D. L. Zhang, Y. H. Wang, T. Z. Qu, and W. K. Li, "Influence analysis of inter band on stability of stratified rockmass," *Chinese Journal of Rock Mechanics and Engineering*, vol. 19, no. 2, pp. 140–144, 2000.

[11] F. L. Guo, D. L. Zhang, J. Su, and X. K. Liu, "Change of strength of surrounding rock system induced by weak interlayer,"

Chinese Journal of Geotechnical Engineering, vol. 31, no. 5, pp. 720–726, 2009.

[12] L. Q. Cao, D. L. Zhang, and Q. Fang, "Semi-analytical prediction for tunnelling-induced ground movements in multi-layered clayey soils," *Chinese Journal of Tunneling and Underground Space Technology*, vol. 102, no. 5, article 103446, 2020.

[13] B. S. Zhang, Y. G. Yan, L. X. Kang, and C. R. Yu, "Application of the contact element method in analyzing the separation and deformation of the stratified roof," *Chinese Journal of Coal Society*, vol. 33, no. 4, pp. 387–392, 2008.

[14] B. S. Zhang, L. X. Kang, and S. S. Yang, "Numerical simulation on roof separation and deformation of full seam roadway with stratified roof and large section," *Chinese Journal of Mining & Safety Engineering*, vol. 23, no. 3, pp. 264–267, 2016.

[15] Q. B. Meng, L. J. Han, W. G. Qiao, D. G. Deng, and S. Y. Wen, "Deformation failure characteristics and mechanism analysis of muddy weakly cemented soft rock roadway," *Chinese Journal of Mining & Safety Engineering*, vol. 33, no. 6, pp. 1015–1022, 2016.

[16] Q. B. Meng, L. J. Han, W. G. Qiao et al., "The deformation failure mechanism and control techniques of soft rock in deep roadways in Zhaolou mine," *Chinese Journal of Mining & Safety Engineering*, vol. 30, no. 2, pp. 165–172, 2013.

[17] Q. Meng, L. Han, W. Qiao, D. Lin, and J. Fan, "Support technology for mine roadways in extreme weakly cemented strata and its application," *International Journal of Mining Science and Technology*, vol. 24, no. 2, pp. 157–164, 2014.

[18] T. C. Li, L. Zhen, J. Z. Liu, and Q. X. Ma, "Deformation and failure process analysis of rectangular roadway in muddy weakly cemented soft rock strata," *Rock and Soil Mechanics*, vol. 35, no. 4, pp. 1077–1083, 2014.

[19] Q. Li and J. Hou, "Research on deformation mechanism and support technology of coal roadway with weakly cemented rock strata in Yangjiacun mine," *Chinese Journal of Coal Engineering*, vol. 48, no. 7, pp. 40–48, 2016.

[20] T. Y. Fan, *Theoretical Basis of Fracture*, Science Press, Beijing, China, 2018.

[21] Z. H. Zhou, *Crack Propagation Mechanism of Fractured Rock under Static-Dynamic Loading and Seepage Water Pressure*, Central South University, Changsha, Hunan, China, 2014.

[22] F. Erdogan and G. C. Sih, "On crack extension in plates under plane loading and transverse shear," *International Journal of Basic Engineering*, vol. 5, no. 4, pp. 512–517, 1963.

[23] R. J. Nuismer, "An energy release rate criterion for mixed mode fracture," *International Journal of Fracture*, vol. 11, no. 2, pp. 245–250, 1975.